

Representation Learning and Identity Adversarial Training for Facial Behavior Understanding

Mang Ning
Utrecht University
m.ning@uu.nl

Albert Ali Salah
Utrecht University
a.a.salah@uu.nl

Itir Onal Ertugrul
Utrecht University
i.onalertugrul@uu.nl

Abstract

Facial Action Unit (AU) detection has gained significant research attention as AUs contain complex expression information. In this paper, we unpack two fundamental factors in AU detection: data and subject identity regularization, respectively. Motivated by recent advances in foundation models, we highlight the importance of data and collect a diverse dataset Face9M, comprising 9 million facial images, from multiple public resources. Pretraining a masked autoencoder on Face9M yields strong performance in AU detection and facial expression tasks. We then show that subject identity in AU datasets provides a shortcut learning for the model and leads to sub-optimal solutions to AU predictions. To tackle this generic issue of AU tasks, we propose Identity Adversarial Training (IAT) and demonstrate that a strong IAT regularization is necessary to learn identity-invariant features. Furthermore, we elucidate the design space of IAT and empirically show that IAT circumvents the identity shortcut learning and results in a better solution. Our proposed methods, Facial Masked Autoencoder (FMAE) and IAT, are simple, generic and effective. Remarkably, the proposed FMAE-IAT approach achieves new state-of-the-art F1 scores on BP4D (67.1%), BP4D+ (66.8%), and DISFA (70.1%) databases, significantly outperforming previous work. We release the code and model at <https://github.com/forever208/FMAE-IAT>, the first open-sourced facial model pretrained on 9 million diverse images.

1. Introduction

The Facial Action Coding System (FACS) was proposed by Ekman for objectively encoding facial behavior through specific movements of facial muscles, named Action Units (AU) [19]. Compared with facial expression recognition (FER) [35, 37, 84] and valence and arousal estimation [52, 55, 85], action units offer a more nuanced and detailed understanding of human facial behavior, because

multiple AUs can occur simultaneously at varying intensities, whereas FER typically involves single-label classification.

This problem attracted considerable interest within the deep learning community [13, 32, 57, 62, 73, 74]. Many works used a facial region prior [13, 39, 57], introduced extra modalities [70, 80, 81], or incorporated the inherent AU relationships [38, 47, 76] to solve the AU detection task and achieved significant advancements. Diverging from these approaches, which often necessitate complex model designs or depend heavily on prior AU knowledge, in this paper, we focus on two fundamental factors that significantly contribute to the AU detection task: data and subject identity regularization, respectively.

Recently, data has become pivotal in training foundation models [2, 42, 58, 65] and large language models [1, 8, 15, 66]. Following this trend, we introduce a large-scale facial dataset Face9M, curated and refined from publicly available datasets, for pretraining. Since most facial tasks require a fine-grained understanding of the face, we propose to do representation learning using Masked Autoencoders (MAE) [27] as masked pretraining results in lower level semantics than contrastive learning [5]. Our large-scale facial representation learning approach demonstrates excellent generalization and scalability in downstream tasks. Notably, our proposed Facial Masked Autoencoder (FMAE), pretrained on Face9M, sets new state-of-the-art benchmarks in both AU detection and FER tasks.

Similar to the importance of data, domain knowledge and task-prior knowledge can be incorporated into the model in the form of regularization [26, 31, 53, 56] to improve task performance. Our key observation is that popular AU detection benchmarks (i.e. BP4D [83], BP4D+ [86], DISFA [51]) have at most 140 human subjects and 192,000 images, which means that each subject has hundreds of annotated images. This abundance can lead models to prefer simple, easily recognizable patterns over more complex but generalizable ones, as suggested by the *shortcut learning theory* [23, 29]. Therefore, we hypothesize that *AU detection models tend to learn the subject identity features to*

infer the AUs, resulting in learning a trivial solution that does not generalize well. To verify our hypothesis, we employed the linear probing technique — adding a learnable linear layer to a trained AU model while freezing the network backbone — to measure identity recognition accuracy. The high accuracy (83%) we obtained clearly shows that the models effectively ‘memorize’ subject identities. To counteract the learning of identity-based features, we propose in this paper Identity Adversarial Training (IAT) for AU tasks by adding a linear identity prediction head and unlearning the identity feature using gradient reverse [20]. Further analysis shows that IAT significantly reduces the identity accuracy of linear probing and leads to better learning dynamics that avoid convergence to trivial solutions. This method further improves our AU models beyond the advantages brought by pretraining with a large-scale dataset.

Although Zhang *et al.* [87] first introduced identity-based adversarial training to AU detection tasks. However, the identity recognition issue and its negative effects have not been explored. Also, the design space of IAT lacks illustration in [87]. We revisit the identity adversarial training method in depth to answer these unexplored questions. In contrast to the weak identity regularization used in [87], we demonstrate that AU detection requires a strong identity regularization. To this end, the linear identity head and a large gradient reverse scaler are necessities for the AU tasks. Our proposed FMAE with IAT sets a new record of F1 score on BP4D (67.1%), BP4D+ (66.8%) and DISFA (70.1%) datasets, substantially surpassing previous work.

Overall, the main contributions of this paper are:

- We demonstrate the effectiveness of using a diverse dataset for facial representation learning.
- We illustrate the identity learning issue and propose the IAT method for AU detection.
- We release the code and checkpoint of FMAE with various model sizes (small, base, large), hoping to facilitate all facial tasks.

2. Related Work

2.1. Action Unit Detection

Recent works have proposed several deep learning-based approaches for facial action unit (AU) detection. Some of them have divided the face into multiple regions or patches [39, 57, 88] to learn AU-specific representations and some have explicitly modeled the relationships among AUs [38, 47, 76]. The most recent approaches have focused on detecting AUs using vision transformers on RGB images [32] and on multimodal data including RGB, depth images, and thermal images [81]. Yin *et al.* [78] have used generative models to extract representations and a pyramid

CNN interpreter to detect AUs. Yang *et al.* [75] jointly modeled AU-centered features, AU co-occurrences, and AU dynamics. Contrastive learning has recently been adopted for AU detection [41, 61]. Particularly, Chang *et al.* [13] have adopted contrastive learning among AU-related regions and performed predictive training considering the relationships among AUs. Zhang *et al.* [80] have proposed a weakly-supervised text-driven contrastive approach using coarse-grained activity information to enhance feature representations. In addition to fully supervised approaches, Tang *et al.* [64] have implemented a semi-supervised approach with discrete feedback. However, none of these approaches have made use of large-scale self-supervised pretraining.

2.2. Facial Representation Learning

Facial representation learning [9, 10, 89] has seen substantial progress with the advent of self-supervised learning [7, 12, 14, 27, 28]. For example, Mask Contrastive Face [69] combines mask image modeling with contrastive learning to do self-distillation, thereby enhancing facial representation quality. Similarly, ViC-MAE [30] integrates MAE with temporal contrastive learning to enhance video and image representations. MAE-face [48] uses MAE for facial pertaining by 2 million facial images. Additionally, ContraWarping [72] employs global transformations and local warping to generate positive and negative samples for facial representation learning. To learn good local facial representations, Gao *et al.* [22] explicitly enforce the consistency of facial regions by matching the local facial representations across views. Different from the above-mentioned work that mainly focuses on models, we emphasize the importance of data (diversity and quantity). Our collected datasets contain 9 million images from various public resources.

2.3. Adversarial Training and Gradient Reverse

Adversarial training [25] is a regularization technique in deep learning to enhance the model’s robustness specifically against input perturbations that could lead to incorrect outputs. Although gradient reverse technique [20] aims to minimize domain discrepancy for better generalization across different data distributions, these two techniques share the same spirit of the ‘Min-Max’ training paradigm and are used to improve the model robustness [21, 36, 49, 67]. Gradient reverse has also been used for the regularization of fairness [59] or for meta-learning [4].

The most relevant research to our paper is [87], where the authors introduce identity-based adversarial training for the AU detection task. However, they did not thoroughly investigate the identity learning phenomenon and its detrimental impacts. Moreover, their empirical settings, the small gradient reverse scaler and the 2-layer MLP identity head, have been [87] verified as an inferior solution to AU detection.

By contrast, we conduct a comprehensive examination for IAT to address these unexplored questions.

3. Methods

3.1. Large-scale Facial MAE Pretraining

While the machine learning community has long established the importance of having rich and diverse data for training, recent successes in foundation models and large language models illustrated the full potential of pertaining [1, 8, 42, 58, 66]. In line with this, our research pivots towards a nuanced exploration of data diversity and quantification in the context of facial representation learning. This approach marks a departure from previous work that predominantly concentrated on refining representation learning algorithms. By prioritizing the scope and scale of data employed for facial pretraining, we aim to uncover more robust and universally applicable facial representations.

We first collect facial images from CelebA [44], FFHQ [33], VGGFace2 [11], CASIA-WebFace [77], MegaFace [34], EDFace-Celeb-1M [79], UMDFaces [6] and LAION-Face [89] datasets, because these datasets contain a massive number of identities collected in diverse scenarios. For instance, the facial images in UMDFaces also capture the upper body with various image sizes, while some datasets (FFHQ, CASIA-WebFace) mainly feature the center face. We then discard images whose width-height-ratio or height-width-ratio is larger than 1.5. Finally, the remaining images are resized to 224*224. The whole process yields 9 million facial images (termed Face9M) which will be used for self-supervised facial pretraining.

Regarding representation learning methods, We apply Masked Image Modeling [27] as it tends to learn more fine-grained features [5] than contrastive learning, which benefits facial behavior understanding. Specifically, we utilize Face9M to train a masked autoencoder (MAE) by the mean squared error between the reconstructed and original images in the pixel space. The decoder of MAE is then discarded for downstream tasks.

3.2. Identity Adversarial Training

One of our key findings in this paper is that, the limited number of subjects in AU datasets makes identity recognition a trivial task and provides a shortcut learning path, resulting in a AU model that contains identity-related features and does not generalize well (see Sec. 5). Motivated by the gradient reverse in domain adaption [20], we propose to apply gradient reverse on AU detection to learn identity-invariant features, aiming at better model generalization.

Our model architecture is presented in Fig. 1, where the backbone is a vision transformer and parameterized by θ_f , the task head predicts the AUs and the ID head outputs the subject identities, respectively. The input image \mathbf{x} is first

mapped by the backbone $G_f(\cdot; \theta_f)$ to a D-dimensional feature vector $\mathbf{f} \in \mathbb{R}^D$, then the feature vector \mathbf{f} is fed into the task head $G_y(\cdot; \theta_{au})$ and the ID head $G_d(\cdot; \theta_{id})$. simultaneously. Assume that we have data samples $(\mathbf{x}, y, d) \sim D_s$, parameters θ_{au} of the task head are optimized to minimize the AU loss L_{au} given AU label y , and parameters θ_{id} of the ID head are trained to minimize the identity loss L_{id} given the identity label d .

To make the feature vector \mathbf{f} invariant to subject identity, we seek the parameters θ_f of the backbone that *maximize* the identity loss L_{id} (Eq. (3)), so that the backbone excludes the identity-based features. In the meantime, the backbone $G_f(\cdot; \theta_f)$ is expected to minimize the AU loss L_{au} . Formally, we consider the following functional loss:

$$L_{au} = \mathbb{E}_{(\mathbf{x}, y) \sim D_s} [CE(G_y(G_f(\mathbf{x}; \theta_f); \theta_{au}), y)] \quad (1)$$

$$L_{id} = \mathbb{E}_{(\mathbf{x}, d) \sim D_s} [CE(G_d(G_f(\mathbf{x}; \theta_f); \theta_{id}), d)] \quad (2)$$

where CE denotes the cross entropy loss function. We seek the parameters $\theta_f^*, \theta_{au}^*, \theta_{id}^*$ that deliver a solution:

$$(\theta_f^*, \theta_{au}^*) = \arg \min_{\theta_f, \theta_{au}} L_{au}(D_s; \theta_f, \theta_{au}) - \lambda L_{id}(D_s; \theta_f, \theta_{id}^*) \quad (3)$$

$$\theta_{id}^* = \arg \min_{\theta_{id}} L_{id}(D_s; \theta_f^*, \theta_{id}) \quad (4)$$

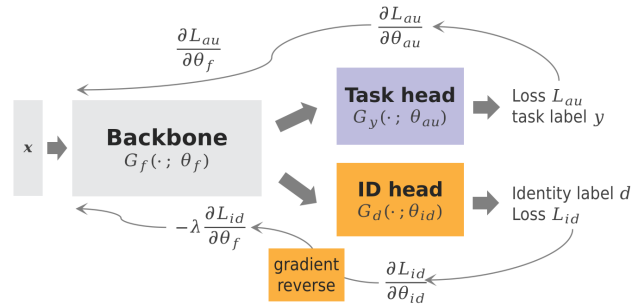


Figure 1. Architecture of Identity Adversarial Training. The task head and ID head both are a linear classifier predicting the AUs and identity, respectively. During training, the task head is optimized by $\frac{\partial L_{au}}{\partial \theta_f}$ and the ID head is optimized by $\frac{\partial L_{id}}{\partial \theta_f}$. The gradient reverse layer multiplies the gradient by a negative value $-\lambda$ to unlearn the features capable of recognizing identities. Finally, the parameters of the backbone are optimized by the two forces: $-\lambda \frac{\partial L_{id}}{\partial \theta_f}$ and $\frac{\partial L_{au}}{\partial \theta_f}$.

where the parameter λ controls the trade-off between the two objectives that shape the feature \mathbf{f} during learning. Comparing the identity loss L_{id} in Eq. (3) and Eq. (4), θ_f is optimized to maximize to increase L_{id} while θ_{id} is learned to reduce L_{id} . To achieve these two opposite optimizations through regular gradient descent and backpropagation, the

gradient reverse layer is designed to reverse the identity partial derivative $\frac{\partial L_{id}}{\partial \theta_{id}}$ before it is propagated to the backbone. The resultant derivative $-\lambda \frac{\partial L_{id}}{\partial \theta_f}$, together with $\frac{\partial L_{au}}{\partial \theta_f}$, are used to update the backbone parameter θ_f .

Intuitively, the backbone is still optimized to learn the AU-related features, but under the force of reducing the identity-related features. The ‘Min-Max’ training paradigm in gradient reverse (see Eq. (3)) resembles the adversarial training [50] and Generative Adversarial Networks (GANs) [24], so we name our method ‘Identity Adversarial Training’ for the AU detection task.

Importantly, we reveal the key design of identity adversarial training for AU detection: *a strong adversarial regularization (large magnitude of $-\lambda \frac{\partial L_{id}}{\partial \theta_f}$) is required to learn identity-invariant features for the backbone.* Specifically, we propose to use a large λ and a linear projection layer for the ID head. The former scales up the $-\frac{\partial L_{id}}{\partial \theta_f}$ and the latter ensures a large L_{id} , leading to a large $\|-\lambda \frac{\partial L_{id}}{\partial \theta_f}\|$ during training. In Sec. 5.3, we will show that the small λ and 2-layer MLP ID head used by [87] would lead to a weak identity regularization (small magnitude of $-\lambda \frac{\partial L_{id}}{\partial \theta_f}$) and inferior AU performance. We defer more details and analysis to Sec. 5.3

4. Experiments

We test the performance of FMAE and FMAE-IAT on AU benchmarks, using the F1 score. To illustrate the generalization of FMAE, we also report its facial expression recognition (FER) accuracy on RAF-DB [60] and AffectNet [54] databases.

4.1. Datasets

BP4D [83] is a manually annotated database of spontaneous behavior containing videos of 41 subjects. There are 8 activities designed to elicit various spontaneous emotional responses, resulting in 328 video clips. A total of 140,000 frames are annotated by expert FACS annotators. Following [39, 70, 80], we split all annotated frames into three subject-exclusive folds for 12 AUs.

BP4D+ [86] is an extended dataset of BP4D and features 140 participants. For each subject, 20 seconds from 4 activities are manually annotated by FACS annotators, resulting in 192,000 labelled frames. We divide the subjects into four folds as per guidelines in [80, 82] and 12 AUs are used for AU detection.

DISFA [51] contains left-view and right-view videos of 27 subjects. Similar to [74, 80], we use 8 of 12 AUs. We treat samples with AU intensities higher or equal to 2 as positive samples. The database contains 130,000 manually annotated images. Following [80] we perform subject-exclusive 3-fold cross-validation.

RAF-DB [60] contains 15,000 facial images with annotations for 7 basic expressions namely neutral, happiness, surprise, sadness, anger, disgust, and fear. Following the previous work [62, 80], we use 12,271 images for training and the remaining 3,068 for testing.

AffectNet [54] is currently the largest FER dataset with annotations for 8 expressions (neutral, happy, angry, sad, fear, surprise, disgust, contempt). AffectNet-8 includes all expression images with 287,568 training samples and 4,000 testing samples. In practice, we only use 37,553 images (from Kaggle) for training as training on the whole training set is expensive.

4.2. Implementation details

Regarding facial representation learning, we pretrain FMAE with Face9M for 50 epochs (including two warmup epochs) using four NVIDIA A100 GPUs. The remaining parameter settings follow [27] without any changes. After the pretraining, we finetune FMAE for FER tasks with cross-entropy loss, and fine-tune FMAE and FMAE-IAT for AU detection with binary cross-entropy loss. In most cases, we finetune the model for 30 epochs with a batch size of 64 and a base learning rate of 0.0005. Following MAE [28], we use a weight decay of 0.05, AutoAugmentation [16] and Random Erasing 0.25 [90] for regularization. By default, we apply ViT-large for FMAE and FMAE-IAT throughout this paper, if not specified otherwise. The complete code, hyperparameters and training/testing protocols are posted on our GitHub repository for reproducibility.

4.3. Result of FMAE

We first show the F1 score of FMAE on the BP4D dataset in Tab. 2. FMAE achieves the same average F1 (66.6%) with the state-of-the-art method MDHR [70] which utilizes a two-stage model to learn the hierarchical AU relationships. Here, we see the effectiveness of data-centric facial representation learning, and demonstrate that a simple vision transformer [18], which is the architecture of FMAE, is capable of learning complex AU relationships. FMAE surpasses all previous work on BP4D+ and DISFA by achieving 66.2% and 68.7% F1 scores, respectively (see Tab. 3 and Tab. 4).

To further verify the importance of the Face9M dataset, we compare FMAE pretrained on Face9M with FMAE pretrained on ImageNet-1k [17], using BP4D as the test set. Figure 2 shows that FMAE pretrained on Face9M always outperforms the one pretrained on ImageNet-1k given the same model size (ViT-base or ViT-large). Also, we empirically demonstrate that FMAE benefits from the scaling effect of model size on AU detection tasks (see the green line in Fig. 2).

In addition to AU detection, we also benchmark FMAE on the downstream facial task of FER. We present the re-

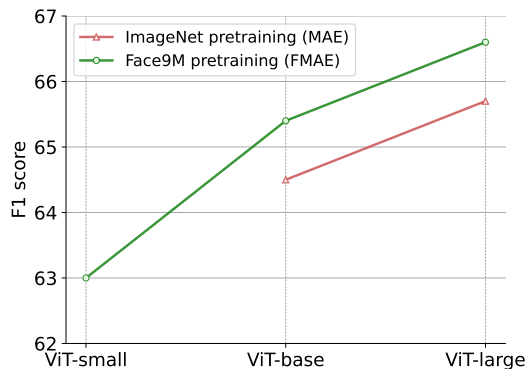


Figure 2. F1 results of FMAE using different model sizes on 12 AUs of the BP4D. Models pretrained on Face9M are better than the ones pretrained on ImageNet-1k. MAE paper does not train ViT-small on ImageNet-1k, thus this entry is missing.

sults of FMAE on AffectNet-8 and RAF-DB in Tab. 1. FMAE sets a new state-of-art accuracy on both datasets (65% on AffectNet-8 and 93.09% on RAF-DB). Note that, we did not test FMAE-IAT on FER tasks because these datasets do not include the identity labels and do not suffer from identity shortcut learning due to the large number of subjects.

Table 1. Results of accuracy on FER benchmarks. FMAE surpasses all previous work.

Methods	Venue	AffectNet-8	RAF-DB
DMUE [62]	CVPR’21	62.84	88.76
EAC [84]	ECCV’22	-	89.99
SOFT [46]	ECCV’22	62.69	90.42
CLEF [80]	ICCV’23	62.77	90.09
LA-Net [71]	ICCV’23	64.54	91.78
FRA [22]	CVPR’24	-	90.76
FMAE	(ours)	65.00	93.09

4.4. Result of FMAE-IAT

Although FMAE has already achieved superior results on AU benchmarks, we highlight that the Identity Adversarial Training could further boost the performance of FMAE across all AU datasets. Specifically, we compare FMAE-IAT with the most recent state of the art methods on BP4D, BP4D+ and DISFA datasets. Tab. 2 suggests that FMAE-IAT shows superior performance by achieving an average F1 Score of 67.1% and FMAE-IAT ranks as the best or second-best performer in several individual AUs, notably AU 1, 2, 4, 12, 17 and 23. Similarly, FMAE-IAT also stands out on BP4D+ dataset with the highest average F1 score

of 66.8%. Our results on the DISFA benchmark are even more distinguishing, FMAE-IAT gains the best or second-best performance on 6 out of 8 AUs, pushing the average F1 score beyond the 70% mark.

For the gradient reverse layer, we use $\lambda = 2.0$ for BP4D, $\lambda = 1.0$ for BP4D+ and $\lambda = 0.5$ for DISFA. Differing from the setting $\lambda \in [0.008, 0.08]$ used in [87], we emphasize that a strong IAT regularization is necessary for AU tasks and we defer the in-depth discussion throughout Sec. 5.

5. Analysis of Identity Adversarial Training

In this section, we elucidate IAT by first showing the identity learning issue in AU tasks (Sec. 5.1), then demonstrating the learning dynamics refined by IAT (Sec. 5.2), and finally illustrating the importance of ensuring a strong regularization of IAT (Sec. 5.3).

5.1. Linear probing for identity recognition

Motivated by the shortcut learning theory [23, 29], we hypothesize that each subject of AU datasets is exposed to the neural network hundreds of times in a single training epoch, which provides an identity shortcut for the model to learn the subject identity. This identity learning issue is undesired, as the model is supposed to generalize to unseen subjects.

To demonstrate the identity learning phenomenon in AU detection, we apply linear probing [14] on a trained AU detection model (FMAE) and evaluate the identity recognition accuracy on the BP4D dataset, which contains 41 subjects. Specifically, we freeze the backbone $G_f(\cdot; \theta_f)$ of a well-trained FMAE and add a learnable linear classifier on top of the backbone to predict the identity label. For each subject in BP4D, we randomly draw 70 samples for training and 30 samples for testing. The resultant accuracy under linear probing is shown in Fig. 3, the red line indicates that FMAE can recognize more than half of people among the 41 subjects even though the model is only trained for one epoch. Given enough training, the identity recognition accuracy can be as high as 83%. By contrast, IAT significantly alleviates this identity learning issue with 4.6% accuracy after one epoch of training and 27.9% accuracy at epoch 19.

An interesting phenomenon is that even under the strong identity unlearning regularization, FMAE-IAT seems still to partially learn the identity-based features, by showing 27.9% accuracy (higher than the random guess accuracy 2.4%). We believe that the inherent high correlation between training and testing images for each subject provides the possibility for the model to infer the identity by looking at the non-face area.

We also visualize the feature output from the backbone of FMAE and FMAE-IAT using t-SNE [68] and see how these features are clustered according to the identity label. Fig. 4 presents the t-SNE results for 20 subjects in BP4D

Table 2. F1 scores (in %) achieved for 12 AUs on BP4D dataset. The best and the second-best results of each column are indicated with bold font and underline, respectively.

Methods	Venue	AU												Avg.
		1	2	4	6	7	10	12	14	15	17	23	24	
HMP-PS [63]	CVPR'21	53.1	46.1	56.0	76.5	76.9	82.1	86.4	64.8	51.5	63.0	49.9	54.5	63.4
SEV-Net [74]	CVPR'21	58.2	50.4	58.3	81.9	73.9	87.8	87.5	61.6	52.6	62.2	44.6	47.6	63.9
FAUT [32]	CVPR'21	51.7	49.3	61.0	77.8	79.5	82.9	86.3	67.6	51.9	63.0	43.7	56.3	64.2
PIAP [64]	ICCV'21	55.0	50.3	51.2	<u>80.0</u>	79.7	84.7	90.1	65.6	51.4	63.8	50.5	50.9	64.4
KSRL [13]	CVPR'22	53.3	47.4	56.2	<u>79.4</u>	80.7	85.1	89.0	67.4	55.9	61.9	48.5	49.0	64.5
ANFL [47]	IJCAI'22	52.7	44.3	60.9	79.9	80.1	<u>85.3</u>	89.2	69.4	55.4	64.4	49.8	55.1	65.5
CLEF [80]	ICCV'23	55.8	46.8	63.3	79.5	77.6	83.6	87.8	67.3	55.2	63.5	53.0	57.8	65.9
MCM [81]	WACV'24	54.4	48.5	60.6	79.1	77.0	84.0	89.1	61.7	59.3	64.7	53.0	60.5	66.0
MDHR [70]	CVPR'24	58.3	<u>50.9</u>	58.9	78.4	<u>80.3</u>	84.9	88.2	69.5	<u>56.0</u>	65.5	49.5	<u>59.3</u>	<u>66.6</u>
FMAE	(ours)	<u>59.2</u>	50.0	<u>62.7</u>	<u>80.0</u>	79.2	84.7	89.8	63.5	52.8	65.1	55.3	56.9	<u>66.6</u>
FMAE-IAT	(ours)	62.7	51.9	<u>62.7</u>	<u>79.8</u>	80.1	84.8	<u>89.9</u>	64.6	54.9	<u>65.4</u>	<u>53.1</u>	54.7	67.1

Table 3. F1 scores (in %) achieved for 12 AUs on BP4D+ dataset. The best and the second-best results of each column are indicated with bold font and underline, respectively. MFT* uses extra depth modality.

Methods	Venue	AU												Avg.
		1	2	4	6	7	10	12	14	15	17	23	24	
ViT [18]	ICLR'21	45.6	38.2	35.5	85.9	88.3	90.3	89.0	81.9	45.8	48.8	57.2	34.6	61.6
CLIP [58]	ICML'21	49.4	39.7	38.9	85.7	87.6	90.6	89.0	80.6	44.9	50.3	56.1	32.8	62.1
SEV-Net [74]	CVPR'21	47.9	40.8	31.2	86.9	87.5	89.7	88.9	82.6	39.9	<u>55.6</u>	59.4	27.1	61.5
MFT [82]	FG'21	48.4	37.1	34.4	85.6	<u>88.6</u>	90.7	88.8	81.0	47.6	51.5	55.6	36.9	62.2
MFT* [82]	FG'21	49.6	42.0	43.5	85.8	<u>88.6</u>	90.6	89.7	80.8	49.8	52.2	59.1	38.4	64.2
CLEF [80]	ICCV'23	47.5	39.6	40.2	86.5	87.3	90.5	89.9	81.6	47.0	46.6	54.3	41.5	63.1
GLTE-Net [3]	Intelli'24	51.5	<u>46.6</u>	43.5	<u>86.8</u>	89.6	<u>91.0</u>	<u>89.8</u>	82.3	46.8	49.3	<u>60.9</u>	50.9	65.7
FMAE	(ours)	<u>53.9</u>	45.5	<u>45.9</u>	86.2	88.3	91.2	89.9	82.3	51.3	56.3	60.7	42.7	<u>66.2</u>
FMAE-IAT	(ours)	54.2	47.0	53.9	85.7	88.4	91.2	89.7	<u>82.4</u>	<u>50.3</u>	54.4	61.0	<u>43.4</u>	66.8

(41 subjects in total), given trained FMAE and FMAE-IAT models. It is clear that the identity-based feature clusters in FMAE become less linearly distinguishable (the ID head is a linear layer) under the effect of IAT.

5.2. F1 learning dynamics

After showing that a regular AU model (FMAE) learns the subject identity, we now illustrate that the identity shortcut learning leads to a trivial AU prediction solution that is inferior to the solution delivered by IAT. Concretely, we observe that FMAE and FMAE-IAT have totally different learning dynamics in terms of AU predictions (indicated by F1 score). Fig. 5 shows the F1 score of both models along the training epochs, where the two models share the same learning rate, batch size and initial training states. It is clear from Fig. 5 that FMAE is optimized quickly and converges at the third epoch with an F1 score of 65.45% under the identity shortcut. In contrast, FMAE-IAT learns the AU decision boundary progressively and converges only at epoch 15 with an F1 score of 66.66%. One can infer that

IAT explicitly pushes the backbone $G_f(\cdot; \theta_f)$ away from the identity-related solution region and delivers a better solution for AU detection tasks.

5.3. Large $\| -\lambda \frac{\partial L_{id}}{\partial \theta_f} \|^2$ is necessary

In Sec. 3.2, we have mentioned the key design space of IAT: a linear projection layer for the ID head and a large λ for the gradient reverse layer. These two factors together ensure the large magnitude of $-\lambda \frac{\partial L_{id}}{\partial \theta_f}$ during the adversarial training of the backbone $G_f(\cdot; \theta_f)$. We elaborate here on the specifics of the IAT design space. We postulate that learning the subject identity is relatively easy, since there are many facial components and non-facial cues that can be used for identity recognition. Therefore, a strong regularization of IAT (i.e., a large $\| -\lambda \frac{\partial L_{id}}{\partial \theta_f} \|^2$) is required to counteract the identity-related learning tendency.

We first show the effect of using different λ on the fold-2 of the BP4D dataset. All models share the same training settings except for λ . In Tab. 5, ‘Epoch’ indicates the train-

Table 4. F1 scores (in %) achieved for 8 AUs on DISFA dataset. The best and the second-best results of each column are indicated with bold font and underline, respectively.

Methods	Venue	AU								Avg.
		1	2	4	6	9	12	25	26	
FAUT [32]	CVPR'21	46.1	48.6	72.8	56.7	50.0	72.1	90.8	55.4	61.5
PIAP [64]	ICCV'21	50.2	51.8	71.9	50.6	54.5	<u>79.7</u>	94.1	57.2	63.8
ANFL [47]	IJCAI'22	54.6	47.1	72.9	54.0	55.7	<u>76.7</u>	91.1	53.0	63.1
KSRL [13]	CVPR'22	60.4	59.2	67.5	52.7	51.5	76.1	91.3	57.7	64.5
KS [40]	ICCV'23	53.8	59.9	69.2	54.2	50.8	75.8	92.2	46.8	62.8
CLEF [80]	ICCV'23	64.3	<u>61.8</u>	68.4	49.0	55.2	72.9	89.9	57.0	64.8
SACL [43]	TAC'23	62.0	65.7	74.5	53.2	43.1	76.9	95.6	53.1	65.5
MDHR [70]	CVPR'24	65.4	60.2	<u>75.2</u>	50.2	52.4	74.3	93.7	58.2	66.2
GPT-4V [45]	CVPRW'24	52.6	56.4	82.9	64.3	55.3	75.4	91.2	66.4	67.3
FMAE	(ours)	62.7	59.5	67.3	55.6	61.8	77.9	95.0	<u>69.8</u>	<u>68.7</u>
FMAE-IAT	(ours)	<u>64.7</u>	61.3	70.8	<u>58.1</u>	<u>59.4</u>	79.9	<u>95.2</u>	71.3	70.1

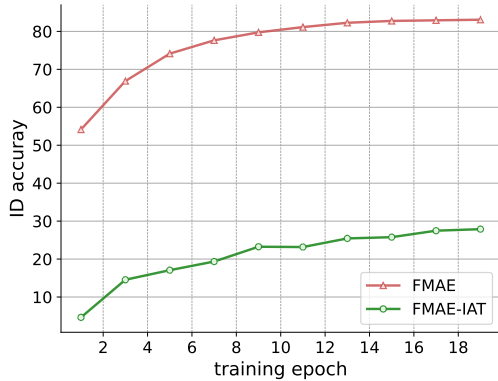
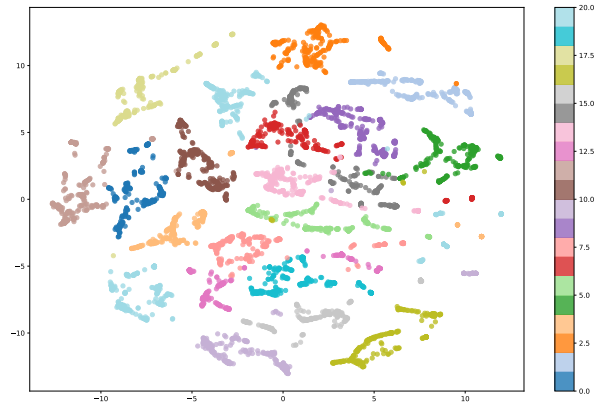


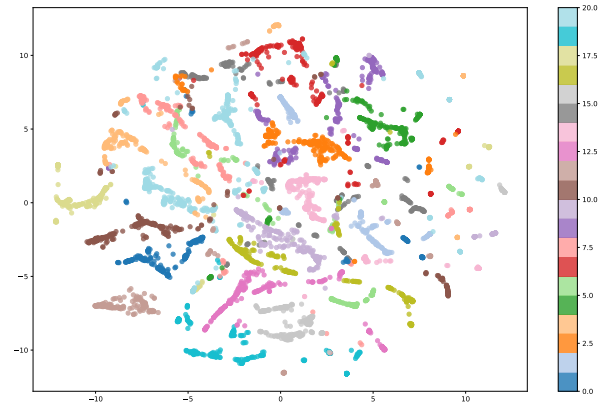
Figure 3. Identity accuracy (%) evaluated by linear probing on the BP4D dataset. IAT greatly reduces the identity-related features learned by the network backbone $G_f(\cdot; \theta_f)$.

ing convergence point in terms of the F1 score and $\lambda = 0$ represents the group without IAT. We see that a small λ ($\lambda = 0.02$), such as the one used in [87], has little gain of F1 score, whereas the large λ ($\lambda = 1, 2, 3$) yields significant improvement of AU prediction. Furthermore, the larger λ we use, the more training epochs are required to reach a better optimization point, which is consistent with the phenomenon in Fig. 5.

Furthermore, we show that recognizing identity is a trivial task since we find that a non-linear ID head $G_f(\cdot; \theta_{id})$ can still recognize the subjects given the identity-invariant features (regularized by IAT). To investigate this in more detail, we increase the model capacity of the ID head $G_f(\cdot; \theta_{id})$ given the backbone trained with a large λ , and measure the identity loss. Tab. 6 shows the results of us-



(a) FMAE



(b) FMAE-IAT

Figure 4. t-SNE visualization of the backbone features on BP4D dataset regarding the identity labels, each color stands for a subject. Only 20 subjects are visualized for readability even though BP4D contains 41 subjects. FMAE features are more identity-clustered than FMAE-IAT features

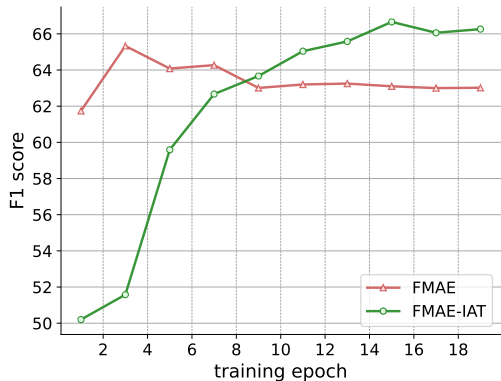


Figure 5. F1 dynamics of FMAE and FMAE-IAT on BP4D+ during training. Fold-2 of BP4D+ is used for visualization.

Table 5. The effect of different λ on BP4D. F1 is reported on fold-2 of BP4D and Epoch means the convergence epoch during training.

λ	0	0.02 (used in [87])	0.2	1	2	3
F1	68.33	68.60	68.63	69.26	69.57	69.47
Epoch	2	10	11	20	21	27

ing different MLP layers for FMAE-IAT under the same regularization strength ($\lambda = 2$). The ID loss in Tab. 6 suggests that the model gradually learns the identity given some model capacity. By contrast, using the 1-layer MLP (linear projection layer) for the ID head leads to a large ID loss L_{id} , thus ensuring the large magnitude of $-\lambda \frac{\partial L_{id}}{\partial \theta_f}$. Therefore the linear projection layer is another necessity for IAT in AU detection. The convergence epoch and F1 score in Tab. 6 also imply that the 2-layer MLP and 3-layer MLP both converge fast and learn a sub-optimal solution to the AU tasks, which is consistent with our previous observations.

Table 6. The effect of different MLPs for the ID head. Epoch in the table shows the convergence epoch during training and ID loss indicates the average identity loss at the convergence epoch using the training set. A higher ID loss implies a lower ID accuracy.

ID head	1-layer MLP	2-layers MLP (used in [87])	3-layers MLP
F1	69.57	69.00	68.90
ID loss	0.152	0.096	0.085
Epoch	21	7	6

6. Conclusion

In conclusion, we have proposed to use a masked auto-encoder (FMAE) with diverse pre-training for the AU detection task in this paper. We have leveraged a vast dataset (Face9M) for pretraining, combined with masked image modeling to significantly improve AU detection performance. Moreover, we have demonstrated the identity learning issue and its harmful effect in AU prediction models. The introduction of Identity Adversarial Training helped in mitigating the model’s learning of identity-related features. Also, We elucidated the two design factors of IAT, and our experiments consistently demonstrated superior performance over previous methods, achieving new SOTA results on AU benchmarks like BP4D, BP4D+ and DISFA.

We also noticed that the scaling effect of FMAE pre-trained on Face9M has not converged even using the ViT-large model, pertaining by ViT-huge and distilling it into a smaller model for practical usage is promising, we leave it to future work.

We provide our trained models and our codebase as open-source to facilitate further research and application development. Note that some ethnicities or age groups may not be represented well in the large dataset. Users should exercise caution while using our pretrained models. Our models should not be used in applications to disadvantage minorities (e.g., develop systems to automatically hire employees by looking at their facial behavior during the interviews).

References

- [1] Josh Achiam, Steven Adler, Sandhini Agarwal, Lama Ahmad, Ilge Akkaya, Florencia Leoni Aleman, Diogo Almeida, Janko Altenschmidt, Sam Altman, Shyamal Anadkat, et al. Gpt-4 technical report. *arXiv preprint arXiv:2303.08774*, 2023. 1, 3
- [2] Jean-Baptiste Alayrac, Jeff Donahue, Pauline Luc, Antoine Miech, Iain Barr, Yana Hasson, Karel Lenc, Arthur Mensch, Katherine Millican, Malcolm Reynolds, et al. Flamingo: a visual language model for few-shot learning. *NeurIPS*, 35:23716–23736, 2022. 1
- [3] Rudong An, Aobo Jin, Wei Chen, Wei Zhang, Hao Zeng, Zhigang Deng, and Yu Ding. Learning facial expression-aware global-to-local representation for robust action unit detection. *Applied Intelligence*, 54(2):1405–1425, 2024. 6
- [4] Marcin Andrychowicz, Misha Denil, Sergio Gomez, Matthew W Hoffman, David Pfau, Tom Schaul, Brendan Shillingford, and Nando De Freitas. Learning to learn by gradient descent by gradient descent. *NeurIPS*, 29, 2016. 2
- [5] Mahmoud Assran, Quentin Duval, Ishan Misra, Piotr Bojanowski, Pascal Vincent, Michael Rabbat, Yann LeCun, and Nicolas Ballas. Self-supervised learning from images with a joint-embedding predictive architecture. In *CVPR*, pages 15619–15629, 2023. 1, 3

- [6] Ankan Bansal, Anirudh Nanduri, Carlos D Castillo, Rajeev Ranjan, and Rama Chellappa. Umdfaces: An annotated face dataset for training deep networks. In *2017 IEEE international joint conference on biometrics (IJCB)*, pages 464–473. IEEE, 2017. 3
- [7] Hangbo Bao, Li Dong, Songhao Piao, and Furu Wei. Beit: Bert pre-training of image transformers. *ICLR*, 2021. 2
- [8] Tom Brown, Benjamin Mann, Nick Ryder, Melanie Subbiah, Jared D Kaplan, Prafulla Dhariwal, Arvind Neelakantan, Pranav Shyam, Girish Sastry, Amanda Askell, et al. Language models are few-shot learners. *NeurIPS*, 33:1877–1901, 2020. 1, 3
- [9] Adrian Bulat, Shiyang Cheng, Jing Yang, Andrew Garbett, Enrique Sanchez, and Georgios Tzimiropoulos. Pre-training strategies and datasets for facial representation learning. In *ECCV*, pages 107–125. Springer, 2022. 2
- [10] Zhixi Cai, Shreya Ghosh, Kalin Stefanov, Abhinav Dhall, Jianfei Cai, Hamid Rezatofighi, Reza Haffari, and Munawar Hayat. Marlin: Masked autoencoder for facial video representation learning. In *CVPR*, pages 1493–1504, 2023. 2
- [11] Qiong Cao, Li Shen, Weidi Xie, Omkar M Parkhi, and Andrew Zisserman. Vggface2: A dataset for recognising faces across pose and age. In *Face and Gesture Recognition*, pages 67–74. IEEE, 2018. 3
- [12] Mathilde Caron, Hugo Touvron, Ishan Misra, Hervé Jégou, Julien Mairal, Piotr Bojanowski, and Armand Joulin. Emerging properties in self-supervised vision transformers. In *ICCV*, pages 9650–9660, 2021. 2
- [13] Yanan Chang and Shangfei Wang. Knowledge-driven self-supervised representation learning for facial action unit recognition. In *CVPR*, pages 20417–20426, 2022. 1, 2, 6, 7
- [14] Ting Chen, Simon Kornblith, Mohammad Norouzi, and Geoffrey Hinton. A simple framework for contrastive learning of visual representations. In *ICML*, pages 1597–1607. PMLR, 2020. 2, 5
- [15] Aakanksha Chowdhery, Sharan Narang, Jacob Devlin, Maarten Bosma, Gaurav Mishra, Adam Roberts, Paul Barham, Hyung Won Chung, Charles Sutton, Sebastian Gehrmann, et al. Palm: Scaling language modeling with pathways. *Journal of Machine Learning Research*, 24(240):1–113, 2023. 1
- [16] Ekin D Cubuk, Barret Zoph, Dandelion Mane, Vijay Vasudevan, and Quoc V Le. Autoaugment: Learning augmentation strategies from data. In *CVPR*, pages 113–123, 2019. 4
- [17] Jia Deng, Wei Dong, Richard Socher, Li-Jia Li, Kai Li, and Li Fei-Fei. Imagenet: A large-scale hierarchical image database. In *CVPR*, pages 248–255. Ieee, 2009. 4
- [18] Alexey Dosovitskiy, Lucas Beyer, Alexander Kolesnikov, Dirk Weissenborn, Xiaohua Zhai, Thomas Unterthiner, Mostafa Dehghani, Matthias Minderer, Georg Heigold, Sylvain Gelly, et al. An image is worth 16x16 words: Transformers for image recognition at scale. *ICLR*, 2020. 4, 6
- [19] Paul Ekman and Erika L Rosenberg. *What the face reveals: Basic and applied studies of spontaneous expression using the Facial Action Coding System (FACS)*. Oxford University Press, USA, 1997. 1
- [20] Yaroslav Ganin and Victor Lempitsky. Unsupervised domain adaptation by backpropagation. In *ICML*, pages 1180–1189. PMLR, 2015. 2, 3
- [21] Yaroslav Ganin, Evgeniya Ustinova, Hana Ajakan, Pascal Germain, Hugo Larochelle, François Laviolette, Mario March, and Victor Lempitsky. Domain-adversarial training of neural networks. *Journal of machine learning research*, 17(59):1–35, 2016. 2
- [22] Zheng Gao and Ioannis Patras. Self-supervised facial representation learning with facial region awareness. In *CVPR*, pages 2081–2092, 2024. 2, 5
- [23] Robert Geirhos, Jörn-Henrik Jacobsen, Claudio Michaelis, Richard Zemel, Wieland Brendel, Matthias Bethge, and Felix A Wichmann. Shortcut learning in deep neural networks. *Nature Machine Intelligence*, 2(11):665–673, 2020. 1, 5
- [24] Ian Goodfellow, Jean Pouget-Abadie, Mehdi Mirza, Bing Xu, David Warde-Farley, Sherjil Ozair, Aaron Courville, and Yoshua Bengio. Generative adversarial networks. *Communications of the ACM*, 63(11):139–144, 2020. 4
- [25] Ian J Goodfellow, Jonathon Shlens, and Christian Szegedy. Explaining and harnessing adversarial examples. *arXiv preprint arXiv:1412.6572*, 2014. 2
- [26] Ishaan Gulrajani, Faruk Ahmed, Martin Arjovsky, Vincent Dumoulin, and Aaron C Courville. Improved training of wasserstein gans. *NeurIPS*, 30, 2017. 1
- [27] Kaiming He, Xinlei Chen, Saining Xie, Yanghao Li, Piotr Dollár, and Ross Girshick. Masked autoencoders are scalable vision learners. In *CVPR*, pages 16000–16009, 2022. 1, 2, 3, 4
- [28] Kaiming He, Haoqi Fan, Yuxin Wu, Saining Xie, and Ross Girshick. Momentum contrast for unsupervised visual representation learning. In *CVPR*, pages 9729–9738, 2020. 2, 4
- [29] Katherine L Hermann, Hossein Mobahi, Thomas Fel, and Michael C Mozer. On the foundations of shortcut learning. *arXiv preprint arXiv:2310.16228*, 2023. 1, 5
- [30] Jefferson Hernandez, Ruben Villegas, and Vicente Ordonez. Vic-mae: Self-supervised representation learning from images and video with contrastive masked autoencoders. *arXiv preprint arXiv:2303.12001*, 2023. 2
- [31] Sergey Ioffe and Christian Szegedy. Batch normalization: Accelerating deep network training by reducing internal covariate shift. In *ICML*, pages 448–456. pmlr, 2015. 1
- [32] Geethu Miriam Jacob and Bjorn Stenger. Facial action unit detection with transformers. In *CVPR*, pages 7680–7689, 2021. 1, 2, 6, 7
- [33] Tero Karras, Samuli Laine, and Timo Aila. A style-based generator architecture for generative adversarial networks. In *CVPR*, pages 4401–4410, 2019. 3
- [34] Ira Kemelmacher-Shlizerman, Steven M Seitz, Daniel Miller, and Evan Brossard. The megaface benchmark: 1 million faces for recognition at scale. In *CVPR*, pages 4873–4882, 2016. 3
- [35] Daeha Kim and Byung Cheol Song. Emotion-aware multi-view contrastive learning for facial emotion recognition. In *European Conference on Computer Vision*, pages 178–195. Springer, 2022. 1

- [36] Alexey Kurakin, Ian Goodfellow, and Samy Bengio. Adversarial machine learning at scale. *arXiv preprint arXiv:1611.01236*, 2016. 2
- [37] Isack Lee, Eungi Lee, and Seok Bong Yoo. Latent-ofer: detect, mask, and reconstruct with latent vectors for occluded facial expression recognition. In *ICCV*, pages 1536–1546, 2023. 1
- [38] Guanbin Li, Xin Zhu, Yirui Zeng, Qing Wang, and Liang Lin. Semantic relationships guided representation learning for facial action unit recognition. In *Proceedings of the AAAI conference on artificial intelligence*, volume 33, pages 8594–8601, 2019. 1, 2
- [39] Wei Li, Farnaz Abtahi, Zhigang Zhu, and Lijun Yin. Eacnet: A region-based deep enhancing and cropping approach for facial action unit detection. In *Face and Gesture Recognition*, pages 103–110. IEEE, 2017. 1, 2, 4
- [40] Xiaotian Li, Xiang Zhang, Taoyue Wang, and Lijun Yin. Knowledge-spreader: Learning semi-supervised facial action dynamics by consistifying knowledge granularity. In *ICCV*, pages 20979–20989, 2023. 7
- [41] Yong Li and Shiguang Shan. Contrastive learning of person-independent representations for facial action unit detection. *IEEE Transactions on Image Processing*, 32:3212–3225, 2023. 2
- [42] Haotian Liu, Chunyuan Li, Qingyang Wu, and Yong Jae Lee. Visual instruction tuning. *NeurIPS*, 36, 2024. 1, 3
- [43] Xin Liu, Kaishen Yuan, Xuesong Niu, Jingang Shi, Zitong Yu, Huanjing Yue, and Jingyu Yang. Multi-scale promoted self-adjusting correlation learning for facial action unit detection. *arXiv preprint arXiv:2308.07770*, 2023. 7
- [44] Ziwei Liu, Ping Luo, Xiaogang Wang, and Xiaoou Tang. Large-scale celebfaces attributes (celeba) dataset. *Retrieved August*, 15(2018):11, 2018. 3
- [45] Hao Lu, Xuesong Niu, Jiyao Wang, Yin Wang, Qingyong Hu, Jiaqi Tang, Yuting Zhang, Kaishen Yuan, Bin Huang, Zitong Yu, et al. Gpt as psychologist? preliminary evaluations for gpt-4v on visual affective computing. In *CVPR*, pages 322–331, 2024. 7
- [46] Tohar Lukov, Na Zhao, Gim Hee Lee, and Ser-Nam Lim. Teaching with soft label smoothing for mitigating noisy labels in facial expressions. In *ECCV*, pages 648–665. Springer, 2022. 5
- [47] Cheng Luo, Siyang Song, Weicheng Xie, Linlin Shen, and Hatice Gunes. Learning multi-dimensional edge feature-based au relation graph for facial action unit recognition. *IJ-CAI*, 2022. 1, 2, 6, 7
- [48] Bowen Ma, Rudong An, Wei Zhang, Yu Ding, Zeng Zhao, Rongsheng Zhang, Tangjie Lv, Changjie Fan, and Zhipeng Hu. Facial action unit detection and intensity estimation from self-supervised representation. *IEEE Transactions on Affective Computing*, 2024. 2
- [49] Aleksander Madry, Aleksandar Makelov, Ludwig Schmidt, Dimitris Tsipras, and Adrian Vladu. Towards deep learning models resistant to adversarial attacks. *arXiv preprint arXiv:1706.06083*, 2017. 2
- [50] Aleksander Madry, Aleksandar Makelov, Ludwig Schmidt, Dimitris Tsipras, and Adrian Vladu. Towards deep learning models resistant to adversarial attacks. In *ICLR*, 2018. 4
- [51] S Mohammad Mavadati, Mohammad H Mahoor, Kevin Bartlett, Philip Trinh, and Jeffrey F Cohn. Disfa: A spontaneous facial action intensity database. *IEEE Transactions on Affective Computing*, 4(2):151–160, 2013. 1, 4
- [52] Liyu Meng, Yuchen Liu, Xiaolong Liu, Zhaopei Huang, Wenqiang Jiang, Tenggao Zhang, Chuanhe Liu, and Qin Jin. Valence and arousal estimation based on multimodal temporal-aware features for videos in the wild. In *CVPR*, pages 2345–2352, 2022. 1
- [53] Takeru Miyato, Toshiki Kataoka, Masanori Koyama, and Yuichi Yoshida. Spectral normalization for generative adversarial networks. In *ICLR*, 2018. 1
- [54] Ali Mollahosseini, Behzad Hasani, and Mohammad H Mahoor. Affectnet: A database for facial expression, valence, and arousal computing in the wild. *IEEE Transactions on Affective Computing*, 10(1):18–31, 2017. 4
- [55] Mang Ning, Itir Onal Ertugrul, Daniel S Messinger, Jeffrey F Cohn, and Albert Ali Salah. Automated emotional valence estimation in infants with stochastic and strided temporal sampling. In *2023 11th International Conference on Affective Computing and Intelligent Interaction (ACII)*, pages 1–8. IEEE, 2023. 1
- [56] Mang Ning, Enver Sangineto, Angelo Porrello, Simone Calderara, and Rita Cucchiara. Input perturbation reduces exposure bias in diffusion models. In *ICML*, pages 26245–26265. PMLR, 2023. 1
- [57] Itir Onal Ertugrul, Le Yang, László A Jeni, and Jeffrey F Cohn. D-pattnet: Dynamic patch-attentive deep network for action unit detection. *Frontiers in computer science*, 1:11, 2019. 1, 2
- [58] Alec Radford, Jong Wook Kim, Chris Hallacy, Aditya Ramesh, Gabriel Goh, Sandhini Agarwal, Girish Sastry, Amanda Askell, Pamela Mishkin, Jack Clark, et al. Learning transferable visual models from natural language supervision. In *ICML*, pages 8748–8763. PMLR, 2021. 1, 3, 6
- [59] Edward Raff and Jared Sylvester. Gradient reversal against discrimination: A fair neural network learning approach. In *2018 IEEE 5th International Conference on Data Science and Advanced Analytics (DSAA)*, pages 189–198. IEEE, 2018. 2
- [60] Li Shan and Weihong Deng. Reliable crowdsourcing and deep locality-preserving learning for unconstrained facial expression recognition. *IEEE Transactions on Image Processing*, 28(1):356–370, 2018. 4
- [61] Ziqiao Shang, Bin Liu, Fei Teng, and Tianrui Li. Learning contrastive feature representations for facial action unit detection. *arXiv preprint arXiv:2402.06165*, 2024. 2
- [62] Jiahui She, Yibo Hu, Hailin Shi, Jun Wang, Qiu Shen, and Tao Mei. Dive into ambiguity: Latent distribution mining and pairwise uncertainty estimation for facial expression recognition. In *CVPR*, pages 6248–6257, 2021. 1, 4, 5
- [63] Tengfei Song, Zijun Cui, Wenming Zheng, and Qiang Ji. Hybrid message passing with performance-driven structures for facial action unit detection. In *CVPR*, pages 6267–6276, 2021. 6
- [64] Yang Tang, Wangding Zeng, Dafei Zhao, and Honggang Zhang. Piap-df: Pixel-interested and anti person-specific fa-

- cial action unit detection net with discrete feedback learning. In *ICCV*, pages 12899–12908, 2021. 2, 6, 7
- [65] Chameleon Team. Chameleon: Mixed-modal early-fusion foundation models. *arXiv preprint arXiv:2405.09818*, 2024. 1
- [66] Hugo Touvron, Thibaut Lavril, Gautier Izacard, Xavier Martinet, Marie-Anne Lachaux, Timothée Lacroix, Baptiste Rozière, Naman Goyal, Eric Hambro, Faisal Azhar, et al. Llama: Open and efficient foundation language models. *arXiv preprint arXiv:2302.13971*, 2023. 1, 3
- [67] Eric Tzeng, Judy Hoffman, Kate Saenko, and Trevor Darrell. Adversarial discriminative domain adaptation. In *CVPR*, pages 7167–7176, 2017. 2
- [68] Laurens Van der Maaten and Geoffrey Hinton. Visualizing data using t-sne. *Journal of machine learning research*, 9(11), 2008. 5
- [69] Yue Wang, Jinlong Peng, Jiangning Zhang, Ran Yi, Liang Liu, Yabiao Wang, and Chengjie Wang. Toward high quality facial representation learning. In *ACM MM*, pages 5048–5058, 2023. 2
- [70] Zihan Wang, Siyang Song, Cheng Luo, Songhe Deng, Weicheng Xie, and Linlin Shen. Multi-scale dynamic and hierarchical relationship modeling for facial action units recognition. In *CVPR*, pages 1270–1280, 2024. 1, 4, 6, 7
- [71] Zhiyu Wu and Jinshi Cui. La-net: Landmark-aware learning for reliable facial expression recognition under label noise. In *ICCV*, pages 20698–20707, 2023. 5
- [72] Fanglei Xue, Yifan Sun, and Yi Yang. Unsupervised facial expression representation learning with contrastive local warping. *arXiv preprint arXiv:2303.09034*, 2023. 2
- [73] Huiyuan Yang, Umur Ciftci, and Lijun Yin. Facial expression recognition by de-expression residue learning. In *CVPR*, pages 2168–2177, 2018. 1
- [74] Huiyuan Yang, Lijun Yin, Yi Zhou, and Jiuxiang Gu. Exploiting semantic embedding and visual feature for facial action unit detection. In *CVPR*, pages 10482–10491, 2021. 1, 4, 6
- [75] Jing Yang, Yordan Hristov, Jie Shen, Yiming Lin, and Maja Pantic. Toward robust facial action units’ detection. *Proceedings of the IEEE*, 111(10):1198–1214, 2023. 2
- [76] Jing Yang, Jie Shen, Yiming Lin, Yordan Hristov, and Maja Pantic. Fan-trans: Online knowledge distillation for facial action unit detection. In *Proceedings of the IEEE/CVF Winter Conference on Applications of Computer Vision*, pages 6019–6027, 2023. 1, 2
- [77] Dong Yi, Zhen Lei, Shengcai Liao, and Stan Z Li. Learning face representation from scratch. *arXiv preprint arXiv:1411.7923*, 2014. 3
- [78] Yufeng Yin, Di Chang, Guoxian Song, Shen Sang, Tiancheng Zhi, Jing Liu, Linjie Luo, and Mohammad Soleymani. Fg-net: Facial action unit detection with generalizable pyramidal features. In *Proceedings of the IEEE/CVF Winter Conference on Applications of Computer Vision*, pages 6099–6108, 2024. 2
- [79] Kaihao Zhang, Dongxu Li, Wenhan Luo, Jingyu Liu, Jiankang Deng, Wei Liu, and Stefanos Zafeiriou. Edface-celeb-1 m: Benchmarking face hallucination with a million-scale dataset. *IEEE TPAMI*, 45(3):3968–3978, 2022. 3
- [80] Xiang Zhang, Taoyue Wang, Xiaotian Li, Huiyuan Yang, and Lijun Yin. Weakly-supervised text-driven contrastive learning for facial behavior understanding. In *ICCV*, pages 20751–20762, 2023. 1, 2, 4, 5, 6, 7
- [81] Xiang Zhang, Huiyuan Yang, Taoyue Wang, Xiaotian Li, and Lijun Yin. Multimodal channel-mixing: Channel and spatial masked autoencoder on facial action unit detection. In *WACV*, pages 6077–6086, 2024. 1, 2, 6
- [82] Xiang Zhang and Lijun Yin. Multi-modal learning for au detection based on multi-head fused transformers. In *Face and Gesture Recognition*, pages 1–8. IEEE, 2021. 4, 6
- [83] Xing Zhang, Lijun Yin, Jeffrey F Cohn, Shaun Canavan, Michael Reale, Andy Horowitz, Peng Liu, and Jeffrey M Girard. Bp4d-spontaneous: a high-resolution spontaneous 3d dynamic facial expression database. *Image and Vision Computing*, 32(10):692–706, 2014. 1, 4
- [84] Yuhang Zhang, Chengrui Wang, Xu Ling, and Weihong Deng. Learn from all: Erasing attention consistency for noisy label facial expression recognition. In *ECCV*, pages 418–434. Springer, 2022. 1, 5
- [85] Yuan-Hang Zhang, Rulin Huang, Jiabei Zeng, and Shiguang Shan. M 3 f: Multi-modal continuous valence-arousal estimation in the wild. In *Face and Gesture Recognition*, pages 632–636. IEEE, 2020. 1
- [86] Zheng Zhang, Jeff M Girard, Yue Wu, Xing Zhang, Peng Liu, Umur Ciftci, Shaun Canavan, Michael Reale, Andy Horowitz, Huiyuan Yang, et al. Multimodal spontaneous emotion corpus for human behavior analysis. In *CVPR*, pages 3438–3446, 2016. 1, 4
- [87] Zheng Zhang, Shuangfei Zhai, Lijun Yin, et al. Identity-based adversarial training of deep cnns for facial action unit recognition. In *BMVC*, page 226. Newcastle, 2018. 2, 4, 5, 7, 8
- [88] Kaili Zhao, Wen-Sheng Chu, and Honggang Zhang. Deep region and multi-label learning for facial action unit detection. In *Proceedings of the IEEE conference on computer vision and pattern recognition*, pages 3391–3399, 2016. 2
- [89] Yinglin Zheng, Hao Yang, Ting Zhang, Jianmin Bao, Dongdong Chen, Yangyu Huang, Lu Yuan, Dong Chen, Ming Zeng, and Fang Wen. General facial representation learning in a visual-linguistic manner. In *CVPR*, pages 18697–18709, 2022. 2, 3
- [90] Zhun Zhong, Liang Zheng, Guoliang Kang, Shaozi Li, and Yi Yang. Random erasing data augmentation. In *AAAI*, volume 34, pages 13001–13008, 2020. 4